Chemical Engineering Journal 151 (2009) 359–366

Contents lists available at ScienceDirect

Chemical Engineering Journal

journal homepage: www.elsevier.com/locate/cej

pH-Responsive composite based on prednisone-block copolymer micelle intercalated inorganic layered matrix: Structure and *in vitro* drug release

Yong Li[a], Hong Li[b], Min Wei[a,*], Jun Lu[a], Lan Jin[a]

[a] *State Key Laboratory of Chemical Resource Engineering, Beijing University of Chemical Technology, Beijing 100029, China*
[b] *China-Japan Friendship Hospital, Beijing 100029, China*

ARTICLE INFO

Article history:
Received 17 November 2008
Received in revised form 22 March 2009
Accepted 26 March 2009

Keywords:
Layered double hydroxides
Prednisone
PTBEM
Micelle
Intercalation
Composite
In vitro release

ABSTRACT

Amphiphilic block copolymer, poly(tert-butyl acrylate-co-ethyl acrylate-co-methacrylic acid), was well established as building block for the preparation of negatively charged micelle, which contains hydrophobic drug prednisone (PNS) in the core. The micelle was further intercalated into galleries of magnesium–aluminum layered double hydroxide (LDH) for the study of drug carrier and release behavior. Powder X-ray diffraction (XRD), Fourier transform infrared (FT-IR) and UV–vis spectroscopy indicate a successful intercalation of PNS-containing micelle between the LDH layers. The scanning electron microscope (SEM) image shows that the as-synthesized drug/polymer–LDH composite exhibits compact microspheres morphology. The release behavior at different pH values was studied in detail, and it was found that the release rate increases with the increase of pH value. Studies on mathematical modeling of drug release show that the system approaches a release mechanism described by approximately Fickian diffusion at pH 7.2 and exhibits anomalous transport at pH 6.4, while it shows the combination of diffusion through the matrix and degradation of the micelle at pH 4.8. The controlled release formulations in this work indicate that this drug-containing composite has potential application in the field of site-specific drug delivery to the colon (pH 7.2), taking advantage of the long transit time and almost complete release.

1. Introduction

Many drugs are only sparingly soluble in water, leading to difficulties in efficient dose delivery and unwanted side effects. Prednisone (PNS, shown in Scheme 1A) is a steroidal anti-inflammatory drug, whose active form is only slightly soluble in water, resulting in poor dispersion in physiological solutions as well as difficulties in efficient dose delivery. Attempts to efficiently deliver PNS or its derivatives involve encapsulation in microspheres, microemulsions, polymeric micelles, and polymeric implants [1–6].

Polymeric drug delivery systems can be used not only to maximize therapeutic activity while minimizing negative side effects, but also to achieve temporal and distribution control in drug therapy. Micelles formed by self-assembly of amphiphilic copolymers combining hydrophilic and hydrophobic segments for drug delivery have attracted much attention because they possess several advantages over other particulate carriers [7–10]. The main advantages include: (1) an increase in water solubility of low soluble or insoluble drugs, and therefore, enhancement of drug bioavailability; (2) protection of drug from deactivation and preservation of its activity during circulation, transport to targeted organ or tissue and intracellular trafficking [11].

Most importantly, the micelle drug carrier can be stimulus responsive by introducing stimulus responsive building blocks into the polymer structure, and these drug carriers made from amphiphilic polymers have drawn tremendous attention over the past decades [12–14]. One area in which these properties have been exploited is targetable delivery of anticancer drugs. The temporal control for a drug therapy could be achieved by the stimuli-responsive property of the hydrophilic segment(s), whereas the distribution control, particularly with respect to the treatment of solid tumor, could be achieved by the cell affinity of the hydrophobic segment(s) via the enhanced vascular permeability of tumor tissue compared to healthy tissue [15].

Oligo(methyl methacrylate) (oMMA) and poly(acrylic acid) (PAAc) are known to be biocompatible materials [16]. This AB block copolymer can form a micellar structure in which a hydrophobic core (oMMA) is surrounded by the bioadhesive polyelectrolyte (PAAc) outer shell. A pH-sensitive carboxylic group in the hydrophobic segment could exert much stronger stimuli-response than that produced by the stimuli-sensitive units in the hydrophilic segment [17]. There is also speculation that pH-sensitive polymeric micelles could be interesting therapeutic carriers since certain pathological

* Corresponding author: Tel.: +86 10 64412131; fax: +86 10 64425385.
E-mail addresses: weimin@mail.buct.edu.cn, weimin-hewei@163.com (M. Wei).

1385-8947/$ – see front matter © 2009 Elsevier B.V. All rights reserved.
doi:10.1016/j.cej.2009.03.049

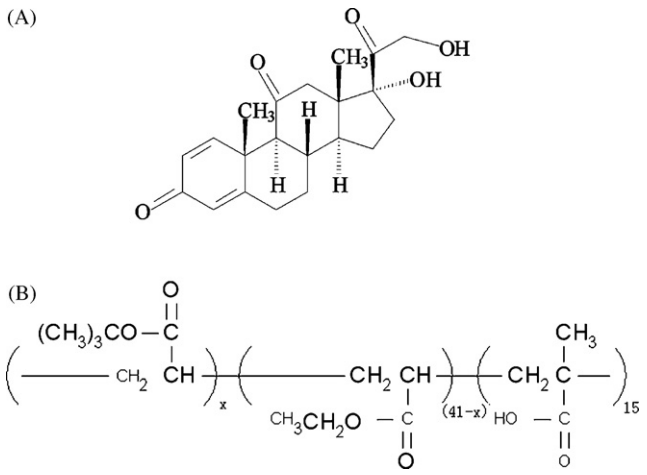

Scheme 1. Chemical structures for (A) PNS and (B) PTBEM.

conditions (i.e. tumors) and cellular compartments (i.e. endosome) are associated with a relatively acidic pH [15,18].

Layered double hydroxides (LDHs), also known as anionic clays, are a class of host–guest layered solids with the general formula $[M^{2+}_{1-x}M^{3+}_{x}(OH)_2]^{x+}A^{n-}_{x/n}\cdot mH_2O$, where M^{2+} and M^{3+} are di- and trivalent metal cations; A^{n-} denotes organic or inorganic anion with negative charge n; m is the number of interlayer water and x ($=M^{3+}/(M^{2+}+M^{3+})$) is the layer charge density of LDHs. Recently, some biocompatible LDHs have attracted considerable attention as drug delivery materials [19,20]. Khan et al. [19] reported that a series of pharmaceutically active compounds can be reversibly intercalated into a layered double hydroxide, and that these materials may have application as the basis of a novel tunable drug delivery system. Gu et al. [21] reported the intercalation of LMWH (low molecular weight heparin) into MgAl-LDH and its dynamical release behavior. Tronto et al. [22] investigated citrate-intercalated MgAl-LDHs and found that the data followed the Higuchi square root law during the release. Li et al. [23] reported that fenbufen-intercalated LDHs as the core was coated with enteric polymers, Eudragit® S100 or Eudragit® L100 as a shell, giving a composite material which shows controlled release of the drug under *in vitro* conditions.

Despite the progress of polymeric drug delivery systems (PDDS), the delivery of active components using clinically approved polymers remains a challenge. Methods such as encapsulation, complexation or covalent conjugation are routinely used in drug delivery research [11]. However, the resulting complexes formed are often unstable in a physiological environment. Meanwhile, most techniques used to achieve specific colonic drug delivery rely on the variation in pH values through the gastrointestinal (GI) tract, although enzymatic degradation by colonic bacteria has been increasingly investigated in recent years [24–26]. The normal transit time [27] in the stomach (pH 1–2) is 2 h (although this may vary) and the transit time in the small intestine is 2–3 h. In order to enhance the stability of polymer–drug micelle and achieve the controlled drug release at the targeted site with the influence of acceptable environmental changes, the immobilization of polymer–drug micelle on a biocompatible LDH matrix is a feasible choice.

In the present study, a new method of controlled PNS delivery system using both polymer and LDH was developed. The method involves two steps: firstly, PNS was encapsulated in an anionic micelle derived from a biocompatible surfactant (poly(tert-butyl acrylate-co-ethyl acrylate-co-methacrylic acid), PTBEM, shown in Scheme 1B); secondly, the negatively charged PNS-loaded micelle was intercalated into galleries of MgAl-LDH by coprecipitation method. The pH-responsive release of this drug/polymer–LDH was studied in detail by the dynamical simulation method. It was found that the release rate increases with the increase of pH value, and a long transit time (up to 78 h) and almost complete release (100%) was obtained at pH 7.2. It can be therefore expected that the controlled release formulation in this work provide potential application in the field of site-specific drug delivery to the colon.

2. Experimental

2.1. Materials

Pyrene, prednisone (PNS) (98% purity) and poly(tert-butyl acrylate-co-ethyl acrylate-co-methacrylic acid) (PTBEM) were purchased from Sigma–Aldrich and used as received. Other analytical grade chemicals including $Mg(NO_3)_2\cdot 6H_2O$, $Al(NO_3)_3\cdot 9H_2O$ and NaOH, were purchased from the Beijing Chemical Co. Limited and used without further purification. Phosphate–citrate buffer solutions were used at 37 °C.

2.2. Characterization of micelle formation

The formation of micelles was confirmed by a fluorescence probe technique using pyrene [16]. The AB block copolymer PTBEM and pyrene were suspended in distilled water, and fluorescence and excitation spectra were measured using a fluorimeter for concentrations of the AB block copolymer varying from 0.0005 to 5 mg/ml. The fluorescence spectrum of pyrene at a fixed excitation wavelength (I_{ex}) of 339 nm, and the excitation spectrum at a fixed emission wavelength (I_{em}) of 393 nm were measured with constant pyrene concentration of 6.0×10^{-7} M.

2.3. Synthesis of NO_3-containing MgAl-LDH

The NO_3-containing MgAl-LDH was synthesized by a procedure similar to that reported previously [28]. A solution of magnesium and aluminum nitrates (molar ratio 2:1) in deionized water, was added dropwise to a solution of sodium hydroxide with vigorous agitation under a N_2 atmosphere. The mixture was aged at 70 °C for 40 h after the solution pH was adjusted to 10. The resulting white precipitate was separated by centrifugation, washed thoroughly with deionized water, and dried at 70 °C for 18 h.

2.4. Synthesis of PNS/PTBEM intercalated LDH nanocomposite

PTBEM was dispersed in water with a concentration slightly above the critical micelle concentration (0.625 g in 200 ml). PNS dispersed in acetone (50 mg in 20 ml) was added to the surfactant solution and stirred at 40 °C under N_2 to allow for the complete evaporation of acetone. An aqueous solution (50 ml) containing NaOH (1.52 g, 0.038 mol) and a solution (50 ml) containing $Mg(NO_3)_2\cdot 6H_2O$ (1.5414 g, 0.006 mol) and $Al(NO_3)_3\cdot 9H_2O$ (1.1306 g, 0.003 mol) (initial Mg/Al = 2.0) were simultaneously added dropwise into the micellar solution under N_2 atmosphere with vigorous stirring until the final pH of ca. 10 was obtained. The resulting slurry was aged at 40 °C for 48 h. The product was filtered, washed with water until the pH close to 7.0, and finally dried in vacuum at room temperature for 24 h. The product was denoted as PNS/PTBEM–LDH.

2.5. Determination of the in vitro drug release rate

The release amount of PNS was measured by UV–vis spectroscopy [29]. A multipoint working curve was made. A series of solutions in simulated gastrointestinal (pH 4.8), the ascending

colon (pH 6.4) and intestinal fluid (pH 7.2) with the concentration of PNS in the range 0–100 ppm were prepared. The UV absorbance of the solution at 243 nm was plotted versus the PNS concentration, and thus linear equations were obtained for the different pH values: conc. = 34.54163*A* + 0.03998, where $R = 0.99975$ (pH 4.8); conc. = 34.6098*A* + 0.00402, where $R = 0.99952$ (pH 6.4); conc. = 34.6498*A* + 0.00412, where $R = 0.99922$ (pH 7.2), respectively.

A known amount of nanocomposite was stirred at the speed of 100 rpm in buffer solution (0.2 M) with specific pH value at 37 °C. In a typical experiment, 0.5 g of the hybrid in 200 ml of buffer solution was used. At specified time intervals, 3 ml of solution was removed and filtered through a 0.2 μm syringe filter. The accumulated amount of PNS released into the solution was measured momentarily using UV–vis spectrophotometer at 243 nm. Runs were performed in triplicate. The release percentage profiles were plotted versus time by using the characteristic absorbance at 243 nm. In order to determine the amount of drug corresponding to total release, Na_2CO_3 (0.53 g) was dissolved in a suspension with the above composition and the mixture was stirred for 2 h (carbonate has a strong affinity for LDHs and can be expected to replace all of the PNS in PNS/PTBEM–LDH by ion-exchange), and the concentration of PNS was also determined by the method described above.

2.6. Characterization

Powder X-ray diffraction (XRD) measurements were performed on a Rigaku D/MAX2500VB2 + /PC diffractometer, using Cu Kα radiation (λ = 0.154 nm) at 40 kV, 200 mA, a scanning rate of 5°/min, and a 2θ angle ranging from 3° to 70°. Fourier transform infrared (FT-IR) spectra were recorded using a Vector 22 (Bruker) spectrophotometer in the range 4000–400 cm^{-1} with 2 cm^{-1} resolution. The standard KBr disk method (1 mg of sample in 100 mg of KBr) was used. UV–vis spectra were recorded on a Shimadzu UV-2501PC spectrometer in the wavelength range 200–700 nm after dissolution of samples in phosphate–citrate buffer solution, and quantitative analysis was performed at 243 nm. The SEM micrograph was recorded on a Hitachi S-3500N scanning electron microscope operating at 20 kV. The sample was dispersed in water thoroughly in an ultrasonic bath, dropped onto quartz glass substrate, and allowed to dry.

3. Results and discussion

3.1. Verification of the formation of PNS-containing micelle

The formation of micelle from the amphiphilic block copolymer was verified by a fluorescence probe technique using pyrene [30]. The fluorescence spectra of pyrene in the presence of the amphiphilic block copolymer (PTBEM) at a fixed I_{ex} of 339 nm are shown in Fig. 1B. It can be seen that the higher the PTBEM concentration, the higher the fluorescence intensity, indicating the formation of micelle.

The excitation spectra of pyrene in the presence of the amphiphilic copolymer at a fixed I_{em} of 393 nm are displayed in Fig. 1A. The peak intensity increases with the increase of the concentration of PTBEM, especially at 339 nm. This is due to the fact that pyrene in water has a very weak absorption at 339 nm, which increases significantly when it is transferred into a hydrophobic environment. This effect also supports the proposed micelle formation. Fig. 2 shows the effect of the PTBEM concentration on the intensity of 393 nm for the emission spectrum. Although the intensity of 393 nm as a function of logarithm of the PTBEM concentration is constant below 316.2 mg/l, it increases dramatically

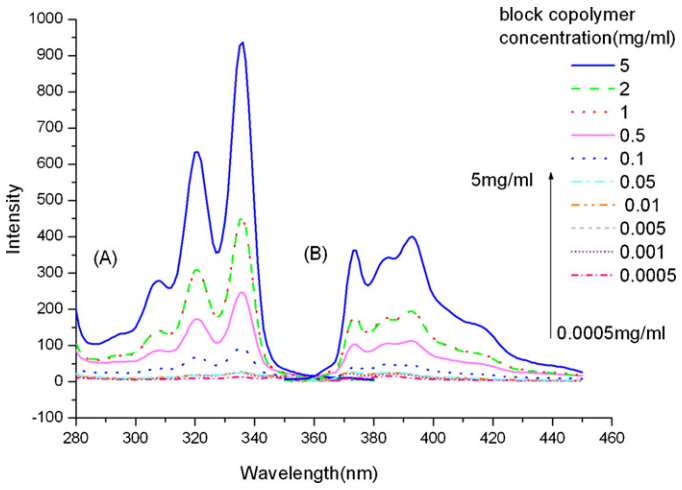

Fig. 1. (A) Excitation spectra of pyrene in the presence of PTBEM at a fixed emission wavelength (I_{em}) of 393 nm. (B) Fluorescence spectra of pyrene in the presence of PTBEM at a fixed excitation wavelength (I_{ex}) of 339 nm. The pyrene concentration was 6.0×10^{-7} M and the concentration of PTBEM was varied from 0.0005 to 5 mg/ml (from bottom to top): 0.0005, 0.001, 0.005, 0.01, 0.05, 0.1, 0.5, 1, 2, 5 mg/ml.

above that concentration, due to the formation of micelles as well as the transfer of pyrene into the hydrophobic domain of the micelle. This concentration can be defined as the critical micellar concentration (CMC). Although the CMC of the amphiphilic block copolymer obtained in this study is higher than that of the poly(N-isopropylacrylamide-b-methyl methacrylate copolymer) micelle (CMC = 50 mg/l) [17], it is much lower than that of typical poloxamers (CMC = 1–24 g/l), indicating that this micelle is relatively stable [16]. Based on the results above, it can be concluded that PTBEM forms micelles in aqueous media with the CMC value of 316.2 mg/l.

3.2. Characterization of PNS/PTBEM–LDH nanocomposite

The powder XRD patterns of the NO_3–MgAl-LDH precursor and the product PNS/PTBEM–LDH are shown in Fig. 3. In each case, the reflections can be indexed to a phase with $R\bar{3}m$ rhombohedral symmetry, commonly used for the description of the LDHs structure [31]. The interlayer distance d_{003} value, representing the combined thickness of the brucite-like layer (0.48 nm) and the gallery height,

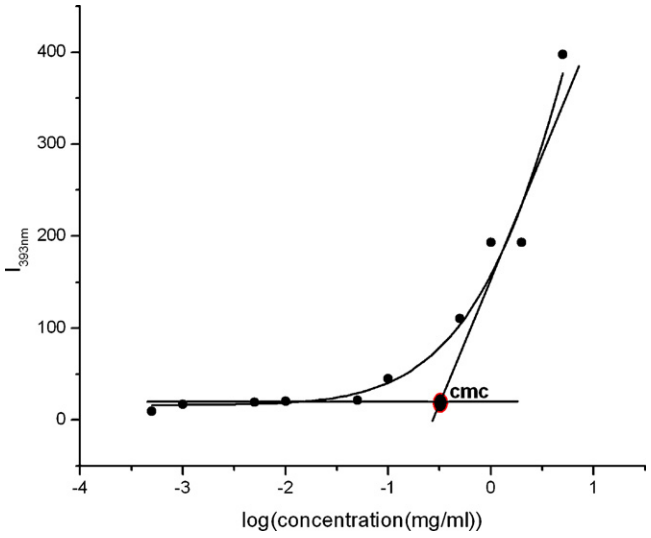

Fig. 2. The intensity of I_{393nm} in the emission spectra as a function of logarithm of PTBEM concentration. $\lambda_{ex} = 339$ nm; [pyrene] = 6×10^{-7} M. The critical micellar concentration (CMC) of micelles self-assembled in aqueous media is 316.2 mg/l.

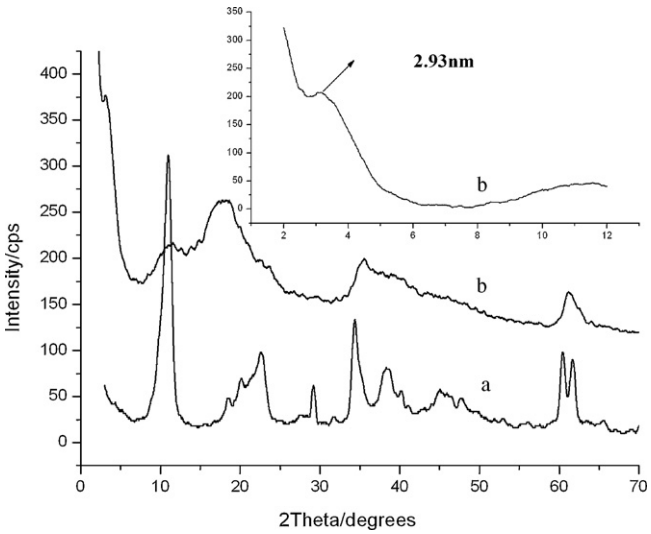

Fig. 3. Powder XRD patterns of (a) NO_3–LDH and (b) PNS/PTBEM–LDH.

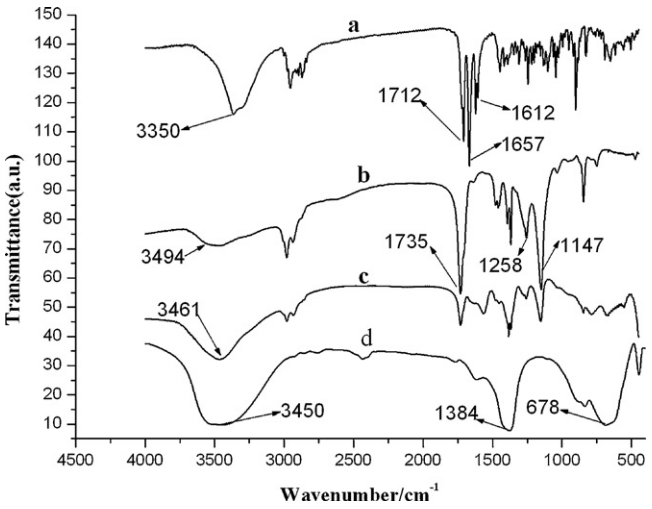

Fig. 5. FT-IR spectra of (a) pristine PNS, (b) pristine PTBEM, (c) PNS/PTBEM–LDH and (d) NO_3–LDH.

is a function of the size and the orientation of intercalated anions. For PNS/PTBEM–LDH nanocomposite (Fig. 3b), the basal reflection (0 0 3) shifts to lower 2θ angles (3.02°, d_{003} = 29.33 Å) compared with that of NO_3–MgAl-LDH (Fig. 3a, 2θ = 10.88°, d_{003} = 8.13 Å), indicating the intercalation of micelle into galleries of LDH. Compared with the NO_3–MgAl-LDH, the crystallinity of the organo-LDH appears to be lower, as shown by the broadening and the decrease in intensity of the XRD signals. Broadness and low intensity of these reflections derive from the disordered layer stacking character of the PNS/PTBEM–LDH nanocomposite and the polydispersity of the interlayer copolymers.

UV–vis spectroscopy was used to investigate whether intercalation of PNS into the LDH host was associated with any change in its chemical composition or environment. Fig. 4 shows the UV–vis spectra of pristine PNS (Fig. 4a), pristine PTBEM (Fig. 4b), the PNS/PTBEM micelle (Fig. 4c), the PNS/PTBEM–LDH composite (Fig. 4d) and PNS released from PNS/PTBEM–LDH after 1 and 8 days (Fig. 4e and 4f), respectively. It can be seen that pristine PNS exhibits a strong absorption band at 243 nm (Fig. 4a), corresponding to the $\pi \rightarrow \pi^*$ transition of the drug, while pristine PTBEM displays no absorption from 200 to 600 nm (Fig. 4b). When PNS was encapsulated into the core of PTBEM micelle, the absorption band of PNS resulting from $\pi \rightarrow \pi^*$ transition shifted to 260 nm (Fig. 4c), with a red-shift of 17 nm compared with pristine PNS in solution. This might be due to the occurrence of the J-aggregation of PNS in the micelle core. Fig. 4d displays that a band at 249 nm was observed for the sample of PNS/PTBEM–LDH composite, indicative of the intercalation of PNS-containing micelle into galleries of LDH. In order to further confirm the existence of drug in the resulting composite, the released PNS from PNS/PTBEM–LDH was also determined. Absorption bands at 246 nm (Fig. 4e) and 240 nm (Fig. 4f) were observed for the released PNS from the PNS/PTBEM–LDH composite, with the intensity becoming dramatically stronger from 1 to 8 days release. The $\pi \rightarrow \pi^*$ transition absorption of the released PNS is very close to the pristine one (243 nm), indicating its approximate molecularity without aggregation. The results above indicate that the PTBEM micelle containing encapsulated PNS was successfully intercalated into the LDH host, which is consistent with the XRD result.

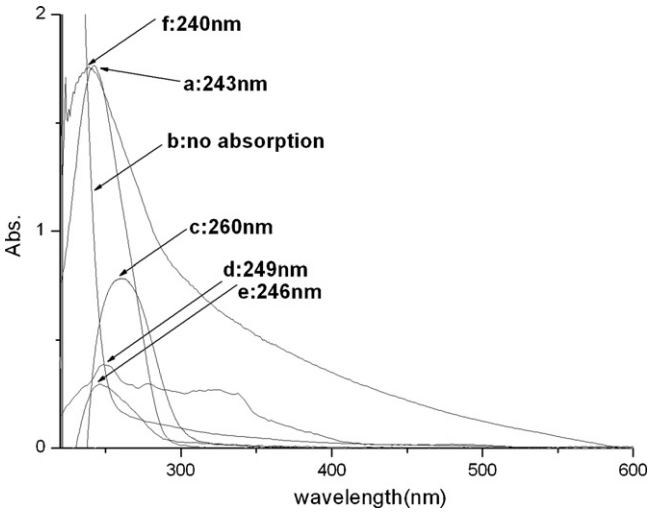

Fig. 4. UV–vis spectra of (a) pristine PNS, (b) pristine PTBEM, (c) PNS/PTBEM micelle, (d) PNS/PTBEM–LDH composite, (e) PNS released from PNS/PTBEM–LDH (1 day), (f) PNS released from PNS/PTBEM–LDH (8 days).

The FT-IR spectra of pristine PNS, pristine PTBEM, PNS/PTBEM–LDH and the NO_3–LDH precursor are shown in Fig. 5. For the sake of clarity, only the main absorption bands were listed. In the spectrum of PNS (Fig. 5a), the band at 3350 cm^{-1} can be attributed to ν(O–H) vibration. The strong absorption bands at 1712 and 1657 cm^{-1} are characteristic of stretching vibrations of ketone group. The band centered at 1612 cm^{-1} is assigned to C=C stretching vibration. The other absorption bands below 1000 cm^{-1} are attributed to δ(C–H) deformation modes. The spectrum of NO_3–LDH precursor (Fig. 5d) shows a broad absorption band at 3450 cm^{-1} due to the stretching vibration of the hydroxyl group in the LDH layers and interlayer water molecules. The band at 1384 cm^{-1} is assigned to the stretching vibration of interlayer NO_3^-. The spectrum of PTBEM (Fig. 5b) shows a broad band (3494 cm^{-1}) corresponding to the stretching vibrations of the OH group of PTBEM. The strong absorption bands at 1147 and 1258 cm^{-1} are characteristic of the asymmetric and symmetric stretching vibrations of O=C–O, respectively. The spectrum of PNS/PTBEM–LDH (Fig. 5c) displays a broad band (3600–3400 cm^{-1}) due to the stretching vibrations of the OH groups in PNS, PTBEM and interlayer water. Moreover, characteristic bands of PTBEM at 1735, 1258, 1147 cm^{-1} were observed, confirming the intercalation of micelle. Although the characteristic bands of PNS were not observed for the sample of PNS/PTBEM–LDH, the UV–vis spectra above demonstrate the presence of PNS in the composite. There are two possible reasons for this result: (1) the movement of

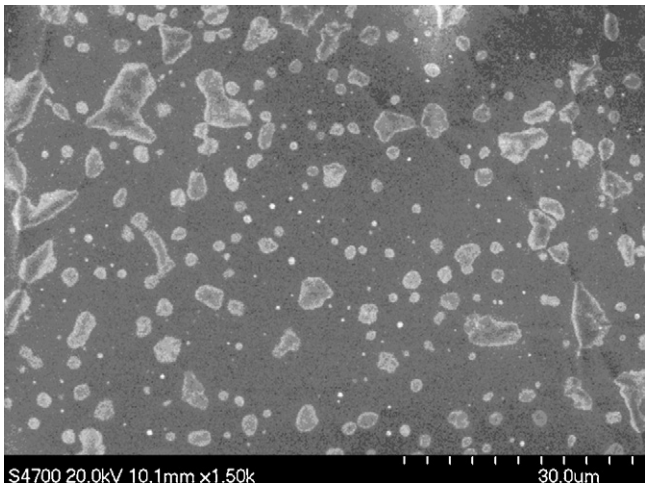

Fig. 6. The SEM image of PNS/PTBEM–LDH.

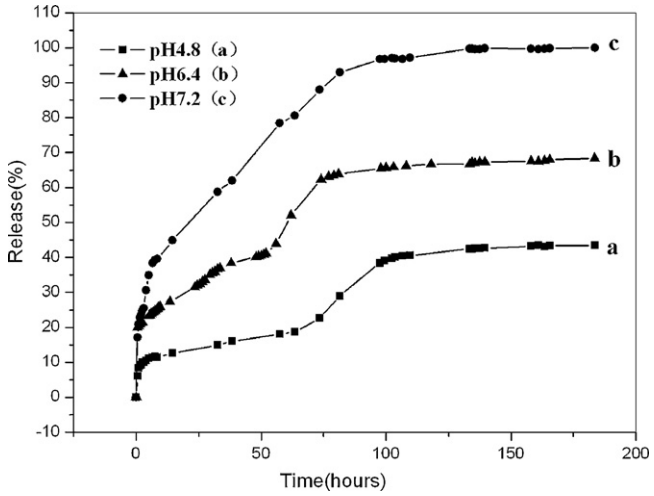

Fig. 7. Release profiles of PNS from the nanocomposite in buffer solutions at different pH values.

encapsulated PNS in the core of PTBEM micelle will be slower in comparison to the movement of drug molecule out of core which is more mobile [17]; (2) the actual concentration of PNS in the PNS/PTBEM–LDH composite is too low to be adequately detected using FTIR spectroscopy.

The morphology of the nanocomposite revealed by SEM is shown in Fig. 6, which presents compact microspheres morphology with particle size of 0.15–1.5 μm. Some agglomerates were also observed due to the modification of LDH surface by organic micelle intercalation.

Based on the basal spacing d_{003} of 2.93 nm for PNS/PTBEM–LDH nanocomposite observed by XRD, the gallery height is calculated to be 2.45 nm by subtracting the thickness of the brucite layer (0.48 nm). By virtue of the presence of carboxyl group of micelle in its structure, it can be proposed that the core/shell micelle (PNS/PTBEM) is accommodated between the galleries of LDH. The interactions in the interlayer region consist of the electrostatic attraction between the positively charged host layers and the negatively charged micelles, as well as the hydrogen bonding formed among the host layers, the guest anions and the interlayer water molecules. A schematic supramolecular structure of PNS/PTBEM–LDH was tentatively proposed and presented in Scheme 2.

3.3. *In vitro* drug release behavior

It has been reported that in the stomach the pH is 1–2; in the lower part of the small intestine (jejunum and ileum) the pH is maintained at 7.5 ± 0.4, then drops to 6.4 ± 0.6 in the ascending colon, and finally rises again to 7.0 ± 0.7 in the distal colon [23]. The ability of PNS/PTBEM–LDH nanocomposite to act an effective controlled release vehicle for intestinal drug delivery was investigated in a series of *in vitro* release experiments by monitoring the time dependence of the concentration of PNS in simulated gastrointestinal and intestinal fluids (pH 4.8, pH 6.4 and pH 7.2).

The *in vitro* release properties of the drug have been investigated by adding the PNS/PTBEM–LDH material to samples of simulated gastrointestinal and intestinal fluid. Fig. 7 shows the release profiles of PNS/PTBEM–LDH in solutions at pH 4.8, pH 6.4 and pH 7.2, respectively, exhibiting that the accumulated PNS released into the buffer solution increases with contact time. It was found that the release rate is faster in the first 10 h from the initial time of the experiment, thereafter a slower release was observed, and equilibrium was achieved after ca. 90 h. In the case of pH 4.8, the percentage of PNS released from hybrid into the buffer solution is the lowest, as shown in Fig. 7a. It was observed that the release amount of PNS was 10% at the end of rapid release step. At equilibrium, it was esti-

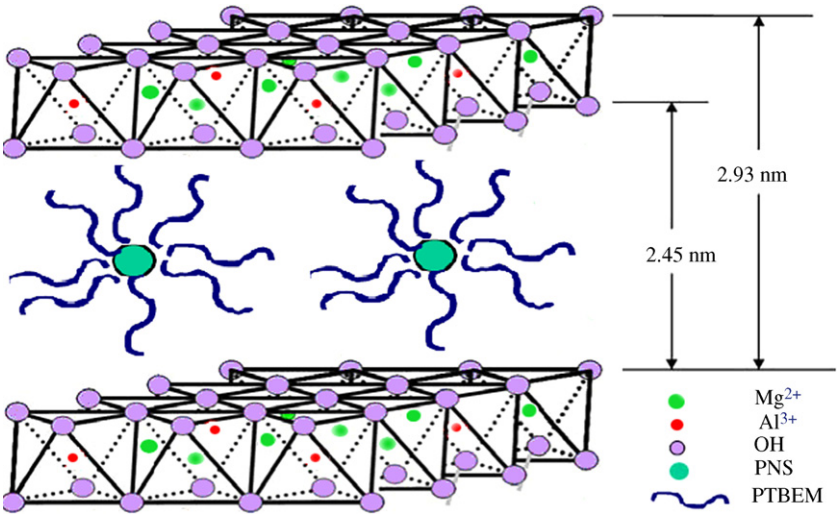

Scheme 2. A possible representation for the structure of PNS/PTBEM–LDH nanocomposite.

mated that 40% of PNS was released from the hybrid into the buffer solution. For pH 6.4, the release amount was 20% and 60% at the end of rapid release step and at equilibrium, respectively. However, the release behavior at pH 7.2 was demonstrated to be the best: almost 100% of PNS could be released from hybrid into the buffer solution at equilibrium.

It can be concluded based on the above results that the order for both the release rate and amount of PNS is pH 7.2 > pH 6.4 > pH 4.8. This is rather different from the release behavior of intercalated drugs upon LDHs reported previously, in which lower pH leads to faster and more complete release of pharmaceutically active components from LDHs [19,21,22,31]. Furthermore, it is worth noticing that the burst release phenomenon at the beginning of release test was inhibited significantly compared with the previous report [19,23,31].

This difference can be explained by the proposed mechanism of drug release from such nanocomposite, which involves an ion-exchange process between guest micelles and phosphate anions in the buffer and then the release of PNS from the micelles. Hence, the following mechanism could be proposed for the release of PNS from the nanocomposite:

(1) Diffusion of the micelle through the nanocomposite: the micelle diffuses from the internal parts of the LDH to the external parts (Fig. 8a).
(2) The micelle situated in the external parts of LDH is exchanged by the phosphate anions in solution (Fig. 8b).
(3) Diffusion of the micelle in the solution (Fig. 8c).
(4) Degradation of the micelle and release of PNS from the core of micelle (Fig. 8d).
(5) Diffusion of the released PNS in the solution (Fig. 8e).

The release rate of PNS from the PNS/PTBEM–LDH nanocomposite into the solution medium will ultimately be determined by the slowest step of these processes. Generally, either step (1) or (4) could be the rate-determining step. This will be further discussed in the next section.

3.4. Mathematical modeling of drug release

The aim of this section is to utilize appropriate mathematical model to verify the hypothesis that the drug release from the nanoparticulate system is either predominantly micelle degradation or diffusion controlled. This would also enable us to calculate drug diffusivities and solubilities for nanoparticulate system, which is a fundamental property of such a system and can prove to be very useful for future studies.

The mechanism of drug release from matrices containing polymer is very complex and not completely understood. Some systems may be classified as either purely diffusion or erosion controlled [32], while others exhibit a combination of these mechanisms [33]. The Korsmeyer–Peppas model (shown in Eq. (1)) was used to analyze drug release from pharmaceutical dosage forms when the release mechanism is not well known or when more than one type of release phenomena is involved [21,34,35].

$$M_r/M_f = kt^n + \alpha \quad (1)$$

Table 1
Interpretation of diffusional release mechanisms from polymeric spherical particles.

Release exponent (n)	Drug transport mechanism	Rate as a function of time
<0.43	Diffusion–erosion	t^{n-1}
0.43	Fickian diffusion	$t^{-0.57}$
0.43 < n < 0.85	Anomalous transport	t^{n-1}
0.85	Non-Fickian	$t^{-0.15}$

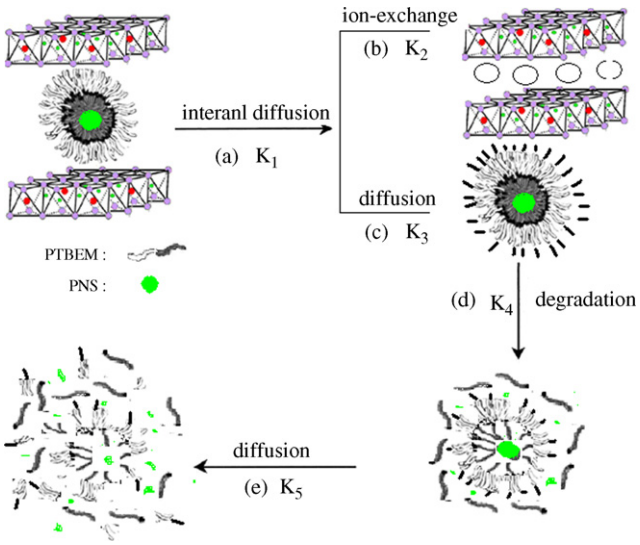

Fig. 8. Schematic representation for the drug release processes of PNS from PNS/PTBEM–LDH nanocomposite in a buffer solution.

where M_r is the release amount of drug at time t; M_f the release amount of drug at infinite time; k the kinetic constant; n an exponent and α represents the drug released at zero time and accounts for the initial burst [36]. The value of n is related to both the geometrical shape of the formulation and the release mechanism. For drug release from spherical particles, the value of n is used in order to characterize different release mechanisms, as listed in Table 1 [34,35,37,38]. The value of n is equal to 0.43 for pure diffusion-controlled release (Fickian diffusion) and 0.85 for pure non-Fickian mechanism; $n < 0.43$ corresponds to the combination of diffusion and erosion control; $0.43 < n < 0.85$ is due to anomalous transport mechanism. Eq. (1) can only be used in systems with a drug diffusion coefficient fairly concentration independent. For the determination of the exponent n, the portion of the release curve where $M_r/M_f < 0.6$ should only be used.

As a result, based on the above theory of drug release from polymeric micro/nanoparticulate systems and according to the release processes in Section 3.3 (Fig. 8), the relationship between n and R (least-squares fit correlation coefficient) was given by Eq. (1) (Fig. 9), and the fitting parameters are tabulated in Table 2. We fit our experimental release data to theoretical release profiles given by Eq. (1) and determined the value of the exponent n so as to test our hypothesis. Fig. 10 shows the theoretical fit to experimental release data for PNS-loaded nanoparticles, in which satisfactory fittings were obtained with coefficient values of 0.98123 (pH 4.8), 0.99698 (pH 6.4) and 0.99602 (pH 7.2). Based on the fitting results above, Korsmeyer–Peppas equations are given below:

$$\text{pH4.8}: M_r/M_f = 7.16677t^{0.230} + 0.44434 \quad (2)$$

$$\text{pH6.4}: M_r/M_f = 1.58646t^{0.680} + 18.63986 \quad (3)$$

$$\text{pH7.2}: M_r/M_f = 15.81623t^{0.386} + 3.07303 \quad (4)$$

As illustrated in Table 2, the solution pH imposes a significant influence on the drug release behavior for the PNS/PTBEM–LDH nanocomposite. The system approaches a release mechanism

Table 2
Fitting parameters of drug release data to Korsmeyer–Peppas model.

pH	k (h^{-n})	n	α	R
4.8	7.16677	0.230	0.44434	0.98123
6.4	1.58646	0.680	18.63986	0.99698
7.2	15.81623	0.386	3.07303	0.99602

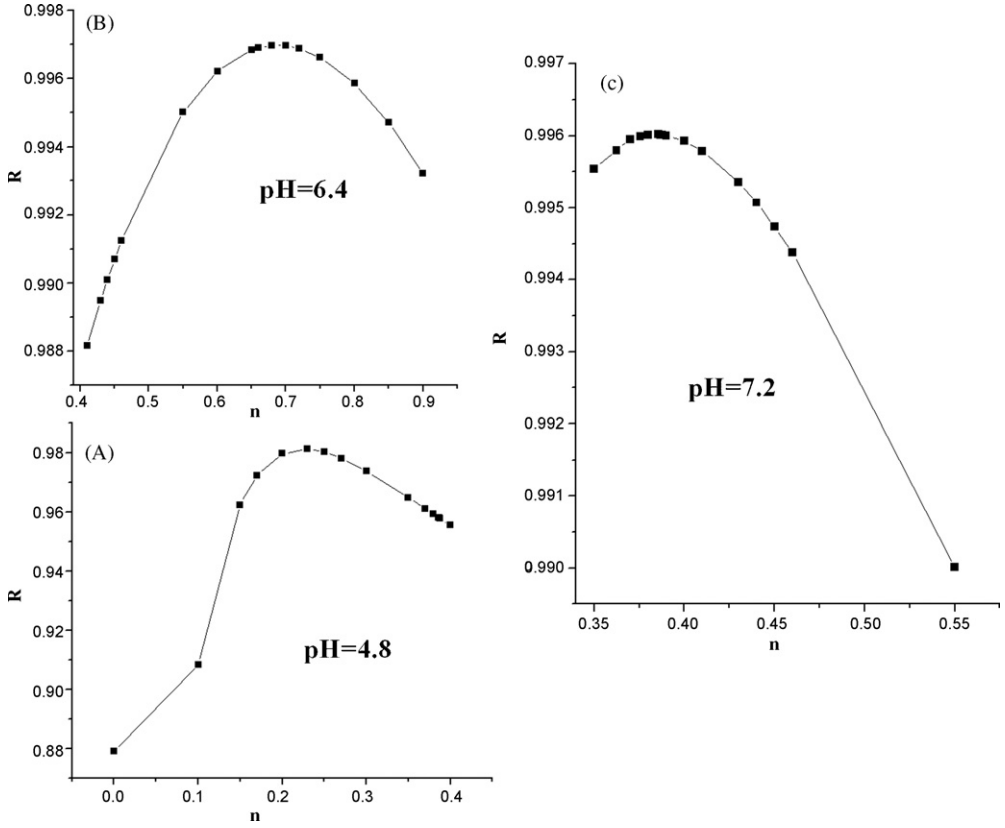

Fig. 9. The relationship between R and n for different release pH values: (A) pH 4.8, (B) pH 6.4 and (C) pH 7.2.

described by the combination of diffusion through the matrix and the degradation of the micelles at pH 4.8 (n = 0.230, Table 2). Anomalous transport can be used to describe the release performance at pH 6.4 (n = 0.680, Table 2), with the lowest kinetic constant k. In the case of pH 7.2, the release behavior fits a mechanism described by approximately Fickian diffusion (n = 0.386, Table 2), with the highest kinetic constant. This is in accordance with the results that the fastest release rate and the highest release amount

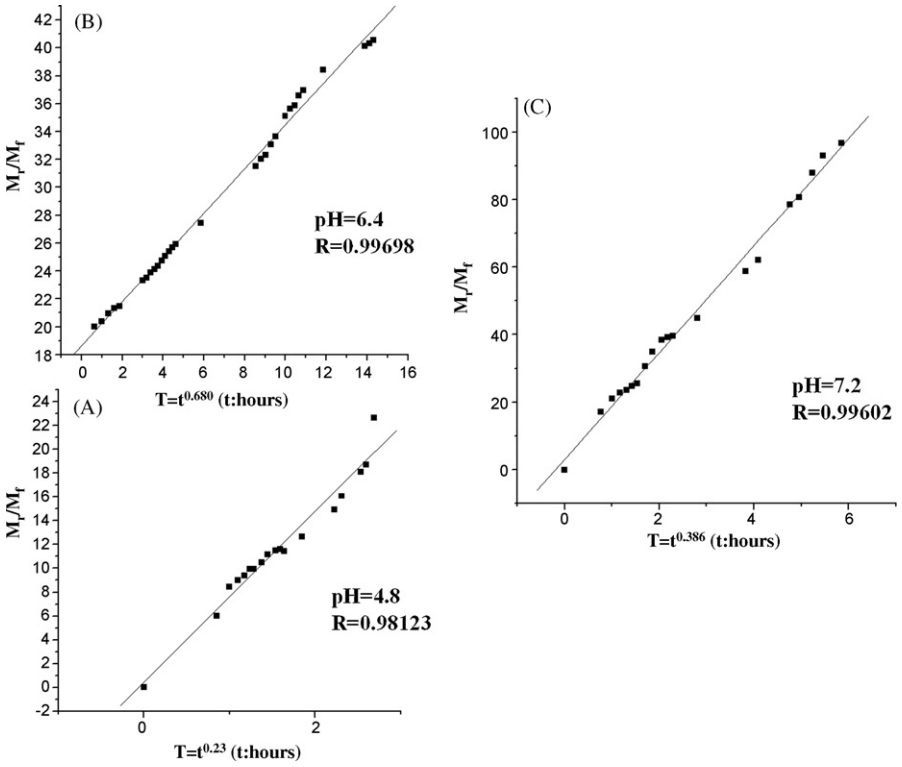

Fig. 10. Plots of Korsmeyer–Peppas kinetic model for the release of PNS from the PNS/PTBEM–LDH nanocomposite: (A) pH 4.8, (B) pH 6.4 and (C) pH 7.2.

of PNS can be obtained at pH 7.2. Therefore, the controlled release study in this work provides a novel pH-responsive drug release formulation, and this drug/polymer–LDH composite can be applied for the site-specific drug delivery to the colon (pH 7.2), by virtue of the long transit time and almost complete release.

4. Conclusions

This work demonstrates a new approach to increase the solubility and prolong the transit time of the therapeutic with the drug/polymer–LDH formulation for site-specific delivery. PTBEM was well established as building blocks for the preparation of negatively charged micelle containing hydrophobic drug PNS, and then the micelle was further intercalated into MgAl-LDH for the study of drug carrier and release. Potentially, the PNS is double protected from the physiological environment, first by the organic environment of the micelle, and second by the durability of the LDH. XRD displays an interlayer distance of 2.93 nm, and FT-IR and UV–vis spectroscopy indicate a successful intercalation of PNS-containing micelle into galleries of LDH. SEM image shows that the as-synthesized drug/polymer–LDH composite possesses compact and non-porous structure with particles size of 0.15–1.5 μm. The intercalated structure of this nanocomposite was proposed. Furthermore, the release behavior at different pH values was studied thoroughly, and it was found that both the release rate and release amount of drug increase with the increase of pH value. This is rather different from the release behavior of pristine drug intercalated LDH, and can be explained by the release mechanism of drug from such nanocomposite, which involves an ion-exchange process between guest micelles and phosphate anions in the buffer and then the release of PNS from the micelles. Mathematical modeling of drug release show that the system approaches a release mechanism described by approximately Fickian diffusion at pH 7.2 and exhibits anomalous transport at pH 6.4, while it shows the combination of diffusion through the matrix and degradation of the micelles at pH 4.8. As a result, the controlled release formulation in this work provides a novel pH-responsive drug release system, and this drug-containing micelle intercalated LDH composite has potential application in the field of site-specific drug delivery to the colon (pH 7.2), taking advantage of the long transit time (up to 78 h) and almost complete release (100%).

Acknowledgments

This project was supported by the National Natural Science Foundation of China, the Program for New Century Excellent Talents in University (Grant No.: NCET-05-121), the 111 Project (Grant No.: B07004) and the 973 Program (Grant No.: 2009CB939802).

References

[1] N. Mennini, S. Furlanetto, F. Maestrelli, S. Pinzauti, P. Mura, Response surface methodology in the optimization of chitosan–Ca pectinate bead formulations, Eur. J. Pharm. Sci. 35 (2008) 318–325.
[2] H. Zhang, S.Y. Tong, X.Z. Zhang, S.X. Cheng, R.X. Zhuo, H. Li, Novel solvent-free methods for fabrication of nano- and microsphere drug delivery systems from functional biodegradable polymers, J. Phys. Chem. C 111 (2007) 12681–12685.
[3] E.S. Brown, A.B. Frol, D.A. Khan, G.L. Larkin, M.E. Bret, Impact of levetiracetam on mood and cognition during prednisone therapy, Eur. Psychiat. 22 (2007) 448–452.
[4] J.P. Karpela, A. Nayakb, W. Lumryc, T.J. Craigd, E. Kerwine, J.E. Fishf, B. Lutskyg, Inhaled mometasone furoate reduces oral prednisone usage and improves lung function in severe persistent asthma, Resp. Med. 101 (2007) 628–637.
[5] L. Weinstock, Z. Hammoud, L. Brandwin, Nonsteroidal anti-inflammatory drug-induced colonic stricture and ulceration treated with balloon dilatation and prednisone, Gastrointest. Endosc. 50 (1999) 564–566.
[6] M.C. Liu, D. Proud, L.M. Lichtenstein, W.C. Hubbard, B.S. Bochner, B.A. Stealey, L. Breslin, H.Q. Xiao, L.R. Freidhoff, J.T. Schroeder, R.P. Schleimer, Effects of prednisone on the cellular responses and release of cytokines and mediators after segmental allergen challenge of asthmatic subjects, J. Allergy. Clin. Immun. 108 (2001) 29–38.
[7] V.P. Torchilin, Structure and design of polymeric surfactant-based drug delivery systems, J. Control. Release 73 (2001) 137–172.
[8] A. Rosler, G.W.M. Vandermeulen, H.A. Klok, Advanced drug delivery devices via self-assembly of amphiphilic block copolymers, Adv. Drug Deliv. Rev. 53 (2001) 95–108.
[9] C. Allen, D. Maysinger, A. Eisenberg, Nano-engineering block copolymer aggregates for drug delivery, Colloids Surf. B Biointerf. 16 (1999) 3–27.
[10] H. Wei, X.Z. Zhang, H. Cheng, W.Q. Chen, S.X. Cheng, R.X. Zhuo, Self-assembled thermo- and pH-responsive micelles of poly(10-undecenoic acid-b-N-isopropylacrylamide) for drug delivery, J. Control. Release 116 (2006) 266–274.
[11] J. Khandare, T. Minko, Polymer–drug conjugates: progress in polymeric prodrugs, Prog. Polym. Sci. 31 (2006) 359–397.
[12] H.S. Mansur, H.S. Costa, Nanostructured poly(vinyl alcohol)/bioactive glass and poly (vinyl alcohol)/chitosan/bioactive glass hybrid scaffolds for biomedical applications, Chem. Eng. J. 137 (2008) 72–83.
[13] L. Li, S.P. Schwendeman, Mapping neutral microclimate pH in PLGA microspheres, J. Control. Release 101 (2005) 163–173.
[14] X.D. Guo, L.J. Zhang, Y. Qian, J. Zhou, Effect of composition on the formation of poly(DL-lactide) microspheres for drug delivery systems: mesoscale simulations, Chem. Eng. J. 131 (2007) 195–201.
[15] X.M. Liu, L.S. Wang, A one-pot synthesis of oleic acid end-capped temperature- and pH-sensitive amphiphilic polymers, Biomaterials 25 (2004) 1929–1936.
[16] T. Inoue, G. Chen, K. Nakamae, A.S. Hoffman, An AB block copolymer of oligo(methyl methacrylate) and poly(acrylic acid) for micellar delivery of hydrophobic drugs, J. Control. Release 51 (1998) 221–229.
[17] H. Wei, X.Z. Zhang, Y. Zhou, S.X. Cheng, R.X. Zhuo, Self-assembled thermoresponsive micelles of poly(N-isopropylacrylamide-b-methyl methacrylate), Biomaterials 27 (2006) 2028–2034.
[18] J. Taillefer, M.C. Jones, N. Brasseur, J.E. Van Lier, J.C. Leroux, Preparation and characterization of pH-responsive polymeric micelles for the delivery of photosensitizing anticancer drugs, J. Pharm. Sci. 89 (2000) 52–62.
[19] A.I. Khan, L. Lei, A.J. Norquist, D. O'Hare, Intercalation and controlled release of pharmaceutically active compounds from a layered double hydroxide, Chem. Commun. (2001) 2342–2343.
[20] G.R. Williams, D. O'Hare, Towards understanding, control and application of layered double hydroxide chemistry, J. Mater. Chem. 16 (2006) 3065–3074.
[21] Z. Gu, A.C. Thomas, Z.P. Xu, J.H. Campbell, G.Q. Lu, *In vitro* sustained release of LMWH from MgAl-layered double hydroxide nanohybrids, Chem. Mater. 20 (2008) 3715–3722.
[22] J. Tronto, M.J.D. Reis, F. Silverio, V.R. Balbo, J.M. Marchetti, J.B. Valim, In vitro release of citrate anions intercalated in magnesium aluminium layered double hydroxides, J. Phys. Chem. Solids 65 (2004) 475–480.
[23] B.X. Li, J. He, D.G. Evans, X. Duan, Enteric-coated layered double hydroxides as a controlled release drug delivery system, Int. J. Pharm. 287 (2004) 89–95.
[24] A. Fetzner, S. Bohm, S. Schreder, R. Schubert, Degradation of raw or film-incorporated β-cyclodextrin by enzymes and colonic bacteria, Eur. J. Pharm. Biopharm. 58 (2004) 91–97.
[25] T. Ugurlu, M. Turkoglu, U.S. Gurer, B.G. Akarsu, Colonic delivery of compression coated nisin tablets using pectin/HPMC polymer mixture, Eur. J. Pharm. Biopharm. 67 (2007) 202–210.
[26] L. Yang, J.S. Chu, J.A. Fix, Colon-specific drug delivery: new approaches and in vitro/in vivo evaluation, Int. J. Pharm. 235 (2002) 1–15.
[27] V.R. Sinha, R. Kumria, Binders for colon specific drug delivery: an in vitro valuation, Int. J. Pharm. 249 (2002) 23–31.
[28] L. Mohanambe, S. Vasudevan, Anionic clays containing anti-inflammatory drug molecules: comparison of molecular dynamics simulation and measurements, J. Phys. Chem. B 109 (2005) 15651–15659.
[29] P.S. Braterman, Z.P. Xu, F. Yarberry, Handbook of Layered Materials, Marcel Dekker, Inc., New York, 2004, pp. 373–380.
[30] K. Kalyanasundoram, J.K. Thomas, Environmental effects on vibronic band intensities in pyrene monomer fluorescence and their application in studies of micellar systems, J. Am. Chem. Soc. 99 (1988) 2039–2044.
[31] M. Wei, M. Pu, J. Guo, J.B. Han, F. Li, J. He, D.G. Evans, X. Duan, Intercalation of L-Dopa into layered double hydroxides: enhancement of both chemical and stereochemical stabilities of a drug through host–guest interactions, Chem. Mater. 20 (2008) 5169–5180.
[32] C. Wischke1, S.P. Schwendeman, Principles of encapsulating hydrophobic drugs in PLA/PLGA microparticles, Int. J. Pharm. 364 (2008) 298–327.
[33] C.R. Young, C. Dietzsch, M. Cerea, T. Farrell, K.A. Fegely, A. Rajabi-Siahboomi, J.W. McGinity, Physicochemical characterization and mechanisms of release of theophylline from melt-extruded dosage forms based on a methacrylic acid copolymer, Int. J. Pharm. 301 (2005) 112–120.
[34] P. Sriamornsak, J. Nunthanid, M. Luangtana-anan, S. Puttipipatkhachorn, Alginate-based pellets prepared by extrusion/spheronization: a preliminary study on the effect of additive in granulating liquid, Eur. J. Pharm. Biopharm. 67 (2007) 227–235.
[35] P. Costa, J.M.S. Lobo, Modeling and comparison of dissolution profiles, Eur. J. Pharm. Sci. 13 (2001) 123–133.
[36] X. Huang, C.S. Brazel, On the importance and mechanisms of burst release in matrix-controlled drug delivery systems, J. Control. Release 73 (2001) 121–136.
[37] K. Kosmidis, E. Rinaki, P. Argyrakis, P. Macheras, Analysis of case II drug transport with radial and axial release from cylinders, Int. J. Pharm. 254 (2003) 183–188.
[38] T. Hayashi, H. Kanbe, M. Okada, M. Suzuki, Y. Ikeda, Y. Onuki, T. Kaneko, T. Sonobe, Formulation study and drug release mechanism of a new theophylline sustained-release preparation, Int. J. Pharm. 304 (2005) 91–101.